

AD-A181 037

FIELD ASSISTED ETCHING(U) ROYAL SIGNALS AND RADAR
ESTABLISHMENT MALVERN (ENGLAND) J A EDWARDS ET AL.
NOV 86 RSRE-MEMO-3715 DRIC-BR-101466

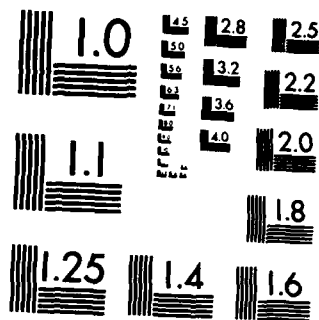
1/1

UNCLASSIFIED

F/G 20/12

NL





MICROCOPY RESOLUTION TEST CHART
NATIONAL BUREAU OF STANDARDS-1963-A

AD-A181 037

ROYAL SIGNALS AND RADAR ESTABLISHMENT

Memorandum 3715

TITLE: FIELD ASSISTED ETCHING

AUTHORS: J A Edwards and J D Benjamin

DATE: November 1986

SUMMARY

We have investigated the effects of both high gravitational and electric fields on wet etching with the objective of inducing anisotropy in otherwise isotropic etch systems and of removing particulates. Although we achieved anisotropy when etching silicon in HNA and gallium arsenide in a phosphoric/sulphuric/peroxide etch in a high gravitational field, the results depended on the size and depth of the features, so we do not believe that this will be useful in standard semiconductor processing. The use of a large gravitational field did result in the removal of a substantial fraction of the particulates which are formed when etching aluminium/silicon/copper, and this may be technologically useful. We also found that the use of large gravitational fields was an effective tool for the identification of diffusion limited etch systems. The application of a high electric field to a prototype non-conducting etch system modified the etching and this effect could merit further investigation.



Copyright
C
Controller HMSO London
1986

Accession For	
NTIS GRA&I	<input checked="" type="checkbox"/>
DTIC TAB	<input type="checkbox"/>
Unannounced	<input type="checkbox"/>
Justification	
By _____	
Distribution/	
Availability Codes	
Dist	Avail and/or Special
A-1	

RSRE MEMORANDUM NO 3715

FIELD ASSISTED ETCHING

J A Edwards and J D Benjamin

CONTENTS

Symbols Used

Introduction

Etching in a Strong Gravitational Field

- 1 Theoretical Results
- 2 Experiments
- 3 Experimental Results
 - i Diffusion Limited Systems
 - ii The Silicon/HNA Etch System
 - iii Particulate Removal from Aluminium Silicon Copper
 - iv Summary of Results
- 4 Discussion

Etching in a Strong Electric Field

- 1 Theoretical Results
- 2 Experiment
- 3 Experimental Results
- 4 Discussion

Conclusions

References

Acknowledgements

Appendix 1 Theory of Etching in a Strong Gravitational Field

Appendix 2 Sources of Error in the Centrifugal Etch Experiments

Appendix 3 Theory of Etching in a Strong Electric Field

Table 1 Etch Systems Investigated

Table 2 Bénard Cell Sizes in the HNA/Silicon System

Table 3 Etch Depth for Various Sample Orientations in the HNA/Silicon System

Table 4 Effect of Increasing Etch Depth on Etch Rate

Table 5 Etching of Gallium Arsenide

Figure 1	Centrifugal Etch Test Mask
Figure 2	Sample in Holder and Bottle
Figure 3	Photograph of Sample Holders and Bottles
Figure 4	Orientations of Sample Relative to Gravity
Figures 5-11	Optical Micrographs of Samples of Silicon Etched with the HNA Etch
Figures 12-13	SEM Profiles of Samples of Silicon Etched with the HNA Etch
Figures 14-15	Micrographs of Etched Gallium Arsenide
Figures 16-17	SEM Micrographs of the Surfaces of Samples of Al/Si/Cu Etched with the Phosphoric Acid Based Etch
Figure 18	Wafer Under Development in an Electric Field
Figures 19-23	SEM Micrographs of PMMA Resist Developed Under Various Electric Fields

SYMBOLS USED

F	Flux
D	Diffusion coefficient
n	Number of a species per unit volume
g	Acceleration due to gravity
μ_g	Gravitational mobility of species
m^*	Difference in mass between species and the medium it displaces
k	Boltzman constant
T	Absolute temperature
η	Viscosity
l	Minimum dimension of cell
$\Delta\rho$	Difference in density of liquid on surface of substrate and in bulk of etch
Ra	Rayleigh number
a	Radius of particle considered
γ	Surface tension
ϵ_0	Permittivity of free space
ϵ_s	Dielectric constant of sphere
ϵ_m	Dielectric constant of medium
v_0	Energy associated with body
E_0	Unperturbed electric field in medium

INTRODUCTION

Apart from orientation dependent etches which depend on the anisotropic etching of a monocrystalline substrate, wet etching is generally considered to be an isotropic process. It follows that the width of etched features must be large compared with their depth. Increasingly, as devices become smaller, this is not what is required, and considerable anisotropy is needed in etching, leading to a move towards plasma etching techniques [1]. However, the equipment necessary for plasma etching is expensive (about £300,000 per etcher), and approaches which could allow satisfactory performance using much deeper wet etching techniques are therefore worth exploring. It has been claimed that etching under a high gravitational field has resulted in anisotropy, in one case producing a ratio of vertical to horizontal etch rates of 10:1, and furthermore it can produce a smoother surface than is normally obtained [2]. Another possible benefit is the removal of particulates which are a problem in some etching systems. We have studied the effects of the application of such a field to a number of common etch systems in order to evaluate its potential use in silicon processing and to gain an insight into the mechanisms of the chemical reactions involved.

We have also investigated the possibility of using strong electric fields to achieve anisotropy in wet chemical etching, both from a theoretical standpoint and experimentally, using the development of PMMA resist in an organic developer as a prototype system.

ETCHING IN A STRONG GRAVITATIONAL FIELD

1 Theoretical Results

The theory of etching in a strong gravitational field is given in detail in Appendix 1. A synopsis of the results is presented below.

In diffusion limited etch systems the rate limiting step in etching is transport of reactants and products to and from the surface. This may be modified by applying a high gravitational field during etching. The gravitational field attainable in an ordinary centrifuge ($g \approx 10^4 \text{ m/s}^2$) is smaller by several orders of magnitude than that required to modify the diffusion of reacting chemicals to a significant degree ($g \approx 10^{11} \text{ m/s}^2$).

However, it is possible to set up convective cells which become the dominant transport mechanism within the etch. Dimensional analysis with typical etch systems and $g \approx 10^4 \text{ m/s}^2$ shows that one might expect to set up convection cells with dimensions down to $10 \text{ }\mu\text{m}$. The exact relationship between the cell size and the dimensions of the features being etched, if the cells are to be important, is not clear, but it seems likely that they will be comparable. It is expected that, in a diffusion limited etch system, convective etching will be associated with an etch rate markedly different from the static etch rate. This could lead to anisotropy in an otherwise isotropic etch if fresh reactants are sucked into the middle of the cell and expelled at the sides. Distinctive cellular flow patterns may be etched on the surface of the substrate.

A further possible benefit concerns removal of particles from the surface. High gravitational fields offer a means of applying a strong force to particles whose density differs from that of their surroundings. Even so, direct removal of a particulate from the substrate during etching is hindered by surface tension. However it should be comparatively easy to remove the particle by dragging it across the surface of the wafer, if the wafer being etched is at an angle to the gravitational field.

2 Experiments

We investigated nominally isotropic etch systems with reactions likely to be diffusion limited; these typically had low activation energies ($\leq 40 \text{ kJ/mol}$, [3]).

The substrates were protected by an etch resistant layer except where a pattern of holes had been opened in it by photolithography and etching. The pattern was defined by the test mask (Figure 1) which comprised a series of circular holes $50\text{--}1000 \text{ }\mu\text{m}$ in diameter and lines and spaces graduating between $0.5 \text{ }\mu\text{m}$ and $400 \text{ }\mu\text{m}$ in width.

The samples were diced into squares of side 15 mm , mounted in PTFE holders (Fig 2,3) and etched in a centrifuge. The holders allowed four different orientations of the face of the sample relative to gravity; this is shown in Fig 4. Samples were centrifugally etched in pairs, each die at a different orientation to gravity. Static controls were also etched.

Care was taken in allowing for temperature variations during the etch. We standardised loading and unloading procedures in order to maximise the reliability of comparisons between samples (see Appendix 2).

The maximum speed at which we ran the centrifuge was 3000 rpm corresponding to a maximum value of $g = 1.9 \times 10^4 \text{ m/s}^2$. Optical and scanning electron microscopes were used to examine etched surfaces. Alpha stepping and scanning electron microscopy (SEM) of scribed cross sections were used to determine etch depths and the extent of undercut.

The substrates in the etch systems studied were silicon, gallium arsenide, silicon dioxide and aluminium silicon copper. Full details of the etch systems are given in Table 1.

3 Experimental Results

1 Diffusion Limited Systems

The data presented in Table 1 show a marked increase in etch rate under strong gravitational fields for the etches used on silicon and gallium arsenide. There were significant differences in etch rate for different orientations of the substrate etched under otherwise similar conditions, and etched flow patterns appeared on the surface of the substrate. Strong gravitational fields appeared to have no effect on the etching of silicon dioxide and aluminium silicon copper. We therefore conclude that the etches we used on silicon and gallium arsenide form diffusion limited systems and those on silicon dioxide and aluminium silicon copper do not. In the case of the etching of silicon dioxide, the low activation energy (of the order of 30 kJ/mole) evidently does not necessarily mean that the reaction is diffusion limited.

11 The Silicon/HNA Etch System

Flow Patterns

We observed flow patterns on the surfaces of samples which had been centrifugally etched. Some flow patterns (for example obvious

'whirlpools' in the ends of the 200 μm and 400 μm lines) were seen on the face up and face up angled orientations but in general the etched surfaces were very smooth, smoother than samples statically etched (Figures 5,6). This we attribute to the prompt removal of gas bubbles during the centrifugal etch.

General pitting of the etched surface due to the establishment of stable Bénard cells was seen in the face down orientation (Figure 7). We also observed this pitting in the face down angled orientation for gallium arsenide (this orientation was not etched for the HNA/silicon system). With the HNA/silicon system, the general appearance of the etched pattern associated with the cell, which we believe reflects the cell structure, was either a raised central area surrounded by a concentric raised ring of about five times the diameter for the larger cells ($\sim 20 \mu\text{m}$ - $\sim 200 \mu\text{m}$ in total diameter), or just a raised central area with the smaller cells ($\sim 5 \mu\text{m}$ to $\sim 20 \mu\text{m}$ in diameter).

The average size of the cell decreased when the depth of the etched feature was increased from about 60 μm (Figure 7) to about 140 μm (Figure 8). However the smallest diameter observed remained about the same at $\sim 5 \mu\text{m}$ (Table 2, Figures 9,10). The smallest cells were observed in the smallest features. This suggests that the value of 'l' obtained in the dimensional analysis (Appendix 1) gives a lower limit to the size of the cell, and its actual size is determined by the local geometry.

The size of the smallest cell increased by a factor of about 5 when the value of g was decreased by a factor of 25 (Table 2, Figures 10,11). Assuming that 'l' is related to the diameter of the cell, this shows that it is difficult to decrease 'l' appreciably by increasing 'g', a result indicated by the dimensional analysis given in Appendix 1.

We believe it reasonable to assume that the features we measured were due to a system of cells which were present for the majority of the etch time. The 'diameter' of the structure was either measured, in the case of large structures, as the diameter of the outer ring, or in the case of small structures, as the distance between one central

feature and the next. The choice of a 'minimum' cell diameter involved picking two cell structures close together and was somewhat subjective. All the measurements in Table 2 were made from figures 7-11.

The Effect of Varying Feature Size within the Sample

From Table 3 it can be seen that for all the orientations and depth etched the 1000 μm diameter hole tended to slope appreciably at the bottom and in general was slightly shallower than the 400 μm diameter hole. The 400 μm , 200 μm and 100 μm holes measured were of roughly the same depth and did not slope appreciably at the bottom. In general they were flatter than the static controls. It was difficult to measure features smaller than 100 μm across with the etch depth we were obliged to use.

For an etch depth of about 80 μm , all the 400 μm lines on the face up angled orientation were fairly uniformly etched to the same depth as the 400 μm hole (there was about a 10% difference between the maximum and minimum measurements of depth), so the circulation patterns set up in the lines at right angles to and along the direction of inclination of the sample were similar. We observed an appreciable amount of slope along the bottom of the 400 μm lines of a sample etched under similar conditions in the face down orientation, with a difference between the maximum and minimum measurements of depth of at least 40%.

The Effect of Varying the Orientation of the Sample Face

In principle it is possible to determine whether the reaction products are denser or less dense than the reactants. The etch rate of one orientation of the sample face should be consistently lower for orientations which trap products than for those which do not, although the situation is less clear cut if both gas and heavy products are formed during the etch. We noted that the silicon/HNA etch system produced bubbles of gas under static conditions.

From a comparison of the depths of the 400 μm holes in those samples etched under high 'g', it can be seen that there is a significant difference in the etch rate between pairs of samples etched in

different orientations. We also observed different types of flow patterns on different orientations. However, whether one orientation etches faster or slower than the other seems to depend on the overall depth of the etched feature. The face up angled orientation was less deeply etched than the face up orientation at an etch depth of about 20 μm , and more deeply etched at about 80 μm , whilst the face up angled orientation is more deeply etched than the face down orientation at about 80 μm and etched to the same depth at about 140 μm . The complex dependence of the etch rate on the etch depth is compatible with there being both gaseous and liquid products and significant changes in the flow patterns with depth.

The Effect of Increasing Etch Depth on Etch Rate

Table 4 indicates that there is some difficulty in setting up convective flow whilst the depth of etched features is less than some critical value 'd'. After this the etch rate is fairly constant.

Static controls show that the lower value of the first etch rate cannot be accounted for by an initial oxide coat on the wafer. It also seems unlikely that the low etch rate for the first sample in the table could only be due to a combination of lower temperature and a proportionally longer time at low fields at the beginning and end of the experiment.

The dimension 'd' is of the order of 10 μm (ie similar to the 'l' discussed above) in the above system. It is difficult to investigate smaller values of etch depth in this system as the etch time under indeterminate 'g' at the beginning and end of the experiment then becomes comparable to that under known 'g' due to the time taken in running up and slowing down the centrifuge.

Observation of Anisotropy

We observed a maximum ratio of vertical to horizontal etch rates of 1.5 ± 0.1 (Figure 12). This was observed on the 200 μm lines on the face up angled orientation with an etch depth of about 80 μm . The face up orientation etched for the same time gave a value for the same ratio

of 1.4 ± 0.1 (Figure 13) whilst the face down orientation etched for the same time showed no significant anisotropy (Figure 13b). These ratios were slightly decreased with samples etched to a depth of about $\sim 140 \mu\text{m}$.

Gallium Arsenide

Gallium arsenide with a silicon dioxide masking layer was etched in 5:5:2 concentrated phosphoric acid: concentrated sulphuric acid: 30% hydrogen peroxide. All orientations were etched. Control of the temperature was difficult because of the tendency of the hydrogen peroxide to decompose exothermically when the etch was poured, but useful results were obtained; they are summarised in Table 5.

Strong cell patterns were established in all samples apart from the face up ones (Fig 14) and the etch rate was substantially higher than in the static case. The bottom of the etched features was generally uneven (but least so for the face up sample), with increased etching often occurring at the sides of the features (Fig 15a). In the case of the angled face up sample, features etched more rapidly on the "uphill" side (Fig 15b). Thus it may be concluded that there was a substantial enhancement in the etch rate due to Bénard cells, but the uniformity of the effect was poor.

iii Evidence of Particulate Removal from Aluminium Silicon Copper

Aluminium silicon copper, which had been deposited by bias sputtering at Plessey Caswell, was etched using the phosphoric acid based etch described in Table 1, with no surfactant. Over a period of 12 minutes a depth of $0.7 \mu\text{m}$ was etched at a temperature of $22-23^\circ\text{C}$ and for those etched in a centrifuge, $g = 1.1 \times 10^4 \text{ m/s}^2$. No evidence of convective etching was found.

The face up, face down and statically etched samples showed many sub-micron sized particles upon their etched surfaces (Fig 16). However photos of samples etched in a face up or face down angled position showed far fewer free particles. Particles tended to collect in the "down field" side of features, and in the case of the face up

orientation, in pits in the surface (Fig 17). Thus there is strong evidence for migration of particles across the surface under the gravitational field.

iv Summary of Results

We were able to distinguish between diffusion limited and non-diffusion limited etching systems.

Etching associated with convective cells was seen under conditions of high gravitational fields in the silicon/HNA system with an enhancement in etch rate over the static case by a factor of about three, and with a cell diameter as small as 5 μm . For holes much greater in diameter than the smallest cell size, the depth of the hole was not strongly dependent on its diameter and the bottoms of the holes, except for the face down orientation, were more level than those statically etched. However, the cells were not in general associated with a high degree of anisotropy, and our experiments indicated that it was both difficult to establish the cells in features shallower than the cell dimension and to decrease this dimension appreciably in a normal centrifuge.

There was evidence for the removal of particulates from aluminium/silicon/copper etched under conditions of high gravitational field.

4 Discussion

The ability to distinguish between diffusion limited and non diffusion limited etch systems by the technique of etching under a high gravitational field is of scientific interest.

Our observations of the effects of etching associated with convective cells in the silicon/HNA system lead us to conclude that the technique of etching under high gravity will not be of use in general silicon processing. This is because the convective cells thus set up are not in general associated with a high degree of anisotropy, both theory and experiment suggest that it will be difficult to reduce the cell dimension to less than a micron, and it is probably difficult to establish them in features whose

depth is much less than this cell dimension. Since the etching depends on a complex flow pattern, the etching is liable to be non-uniform and difficult to predict in advance. However, the technique may be of use in specialised applications such as the production of very smooth surfaces and the deep etching of simple and fairly coarse features such as vias through wafers [4].

We have demonstrated a promising approach to the removal of particulates from aluminium silicon copper during wet etching.

ETCHING IS A STRONG ELECTRIC FIELD

1 Theoretical Results

We have already investigated the effects of the application of a high gravitational field during wet etching. However electrical forces in practicable systems are generally much greater than gravitational forces. For example, whereas the gravitational force on a molecule of mass 4×10^{-26} kg in a gravitational field of 10^4 m/s² is 4×10^{-22} N, the force on a charge of 'e' in an electric field of 10^6 V/m is 2×10^{-13} N which is 5×10^8 times larger.

There are two possible effects which strong electric fields can have on the transport of reactants and etch products in the diffusion layer of the etch. The first is that variations in the dielectric constant between reacted and unreacted etch will lead to directional diffusion of molecules into and out of regions of high electric field, and also to the setting up of convection cells. This effect is however no stronger than the effect of strong gravitational fields (Appendix 3). A second effect is that if the reactants or solvated species carry a net charge of even a fraction of an electronic charge, the electric field will pull them towards or away from the interface. This effect can be very strong.

The use of electric fields to assist etching is however only applicable to the etching of non-conducting materials using non conducting etches. Ionic etches will both screen the electric field close to the interface so that the electric field will not penetrate into the etch, and will also electrolyse if a dc or low frequency field is used. If the material being etched is conducting, the electric field will be normal to the surface on a

microscopic scale, and the effect due to the electric field will be isotropic. This leaves the etching of dielectrics and resists using organic etches. As a prototype system we investigated the effect of a strong dc electric field on the development of PMMA resists in a non-conducting organic developer, both to see what effect was produced and to determine whether it might assist in the development of very small ($\sim 1 \mu\text{m}$) resist features.

2 Experiment

We performed a quick experiment to see whether any large improvement was obtained in the development of resist features about a micron across under an electric field.

A layer of PMMA about 1 micron thick was deposited on one side of a number of 2" silicon slices and exposed to an E-beam. The test patterns used were the RSRE resolution test pattern and a series of thin parallel lines. Two wires were then glued with silver loaded epoxy to the back of each slice and developed under an electric field as shown in Figure 19. The electrode was a chrome gold plated silicon wafer. The resist slice was held face down by a weight upon microscope cover slips which acted as spacers between it and the electrode. A dc bias of about 250 V was applied between the electrode and the resist coated wafer, and was measured with a voltmeter in a four terminal arrangement. The developer used was a mixture of equal parts of isobutyl methyl ketone (IBMK) with isopropyl alcohol (IPA) and conducted only slightly.

The distance between the electrode and the resist slice was 0.4 mm so 250 V gave an average electric field of $6.25 \times 10^5 \text{ V/m}$. The actual values of the electric field in the resist and developer were not known, but since the resistivity of the resist may have differed significantly from that of the developer, it was unlikely that the electric field was the same in both the developer and the resist.

Each slice was developed for 70 s, most of this time with the field on. It was then rinsed with agitation for 20 s each in two beakers of clean IPA. Controls were also developed in exactly the same way but with no field applied. The temperature at which they were developed was about 20°C.

3 Results

We developed one sample (A) with the positive plate as the electrode and one sample (B) with the positive plate as the resist slice. For both these the temperature was 18°C. We also developed a control with no field applied.

On comparison of the 5 μm , 2 μm and 1 μm lines we found that sample (A) was significantly better developed than sample (B), and had developed slightly better than the control (figures 19-21). Also with the small chequerboard patterns exposed at this frequency, it seemed that (A) was better developed than (B) (figures 22-23).

On examining the gold counterelectrode after the development of samples (A) and (B) the resist pattern was seen on its surface. This disappeared with rinsing and agitation with fresh developer.

In view of lack of time, we were not able to repeat the experiment to our satisfaction.

4 Discussion

These preliminary results indicate that the development of resist is indeed affected by an electric field. The results are, however, fairly tenuous and their reproducibility is uncertain. It does however appear that the use of large electric fields to modify etching merits further investigation. This might best be done with a simpler prototype system, eg looking at the dissolution of a polymer which is protected by a patterned masking layer into a one component solvent. This would eliminate uncertainties associated with the electron beam exposure and possible segregation of components of the etch under the electric field.

CONCLUSIONS

We have demonstrated centrifugal etching under high 'g' with silicon as substrate and conclude that it may be of use in the investigation of

reaction mechanisms and the deep etching of large features but not in everyday silicon processing.

We have also demonstrated a promising approach to the removal of particulates from aluminium silicon copper during wet etching.

The results of our experiments on the effects of electric fields on resist development suggest that the field had an effect on the development of features of the order of 1 μm in width and that the effects of strong electric fields on etching could merit further investigation.

REFERENCES

- 1 V G I Deshmukh, T I Cox and J D Benjamin. 'Silicon microetching technology'. Phys Technol Vol 15, 1984, p 301.
- 2 H K Kuiken and R P Tijburg. 'Centrifugal Etching, A Promising New Tool to Achieve Deep Etching Results". J Electrochemical Soc, August 1983, p 1722.
- 3 W Kern. 'Chemical Etching of Si, Ge, GaAs, GaP'. RCA Review Vol 39, June 1978, p 278.
- 4 J D Benjamin, A L Mears and A S R Martin. 3D Integrated Circuit Chipstacks. RSRE Memorandum 3960, 1986.

ACKNOWLEDGEMENTS

We are indebted to the staff of SPEL, Caroline Vizard, Heather Willis, Ted Jackson, M Bennet, Doug Brumhead, Martin Hepplewhite, George Gibbons and Simon Mortimer for all their help, and to John White, John Woodward, Philip Tufton, Alan Brown and Vincent Mifsud for useful discussions.

APPENDIX 1

THEORY OF ETCHING IN A STRONG GRAVITATIONAL FIELD

The presence of a large gravitational field can in principle have three effects on etching. Firstly it provides a potential gradient which might modify diffusion. Secondly it may set up convection cells which will take over from diffusion as a mechanism by which material is transported from the surface into the bulk of the etchant. Finally it may assist in the removal of gas bubbles and particulates from the surface of the material. These processes are discussed below.

The flux of material diffusing away from a surface,

$$f = D \frac{dn}{dz} + gn \mu_g$$

where D is the diffusion coefficient, n is the number of species per unit volume, g is the value of gravity and μ_g is their gravitational mobility. μ_g is related to D by an Einstein relation:

$$\mu_g = \frac{m^* D}{kT}$$

where m^* is the difference in mass between the species and the medium it displaces. So,

$$F = D \left(\frac{dn}{dz} + \frac{gnm^*}{kT} \right) = Dn \left(\frac{d \ln(n)}{dz} + \frac{gm^*}{kT} \right)$$

The artificial gravitational field will be of importance if

$$\frac{gm^*}{kT} > \frac{d \ln(n)}{dz}$$

Typically for an inorganic etch, $m^* = 2 \times 10^{-26}$ kg, $T = 300$ K and $\frac{d \ln(n)}{dz} = 10^6 \text{ m}^{-1}$ so this implies $g > 2 \times 10^{11} \text{ m/s}^2$. This is prohibitive, so normally this mechanism will only be important if m^* is made very large, for example if the material being removed is a long chain organic molecule, and $d \ln(n)/dz$ is made very small by using an etch solution which already contains a high concentration of reaction products. Then if $m^* = 2 \times 10^{-23}$ kg (corresponding to an organic molecule of RMM $\approx 12,000$) and

$d \ln(n)/dz$ is 100, a value of $g \sim 2 \times 10^4 \text{ m/s}^2$ (attainable in an ordinary centrifuge) is needed to etch small features anisotropically. This effect may be useful in the development of resists where large RMM long chain molecules (for example PMMA, RMM $\approx 30,000$ – $150,000$) may dissolve into almost saturated solutions. However, if an effect of this type were desired it could probably be achieved much more easily by means of an electric field.

The second mechanism (that discussed by Kuiken and Tjburg (1)) depends on convective cells becoming the dominant transport mechanism. Provided that it is assumed that the only important quantities in determining when the cells become dominant are the diffusion coefficient D , viscosity η , cell size d and $g\Delta\rho$ where g is the effective value of gravity and $\Delta\rho$ is the difference in density of the liquid on the surface and in the bulk of the solution, dimensional analysis indicates that the behaviour of the system depends on the value of the dimensionless quantity $\frac{g\Delta\rho d^3}{\eta D}$, known as the Rayleigh number (Ra). For most aqueous systems $D \sim 10^{-9} \text{ m}^2/\text{s}$ and $\eta \sim 10^{-3} \text{ Nsm}^{-2}$ and $\Delta\rho$ is typically 10 kg m^{-3} , so for $10 \text{ }\mu\text{m}$ features $Ra \approx 100$ (regarded as typical of the onset of convection) will occur when $g \sim 10^4 \text{ m/s}^2$ which should be readily achieved.

One important uncertainty is the relation between feature size and l . This cannot be determined from this analysis although one would expect it to be related to the cell size.

Once established, for systems in which the reaction rate is diffusion limited, the convection cells may cause an increase in the effective etch rate in systems etched under high gravity over those statically etched. This may be accompanied by a reduction in relative undercut, ie anisotropic etching may be induced. If an increase in etch rate does occur, we would expect to see different etch rates between similar features etched at different orientations relative to gravity as a result of the different circulation patterns established within them. We might also expect to see a strong dependence of etch rate on feature size. Distinctive cellular structures due to Bénard cell circulation patterns may form in features etched under a high field pointing away from the face of the substrate.

The third effect may be particle removal. Once a body is detached from the surface it should fall at a speed determined by its weight and viscous

drag, so once particles are detached a large gravitational field should greatly speed their departure. This leaves the problem of causing the particles to become detached in the first place. The chief factor preventing this is surface tension(γ), since as the particle leaves the substrate, extra surface area of liquid will be formed roughly equal to the distance by which the particle has moved multiplied by the perimeter of the area over which the particle prevents the liquid from touching the surface of the substrate. Thus, assuming that the perimeter is the same as that of the particle (a pessimistic assumption), a spherical particle of radius 'a' is held on to the surface by a force of roughly $2\pi a\gamma$. If gravity points normally away from the surface, the particle will be pulled away by a force of roughly $\frac{4}{3}\pi a^3\Delta\rho g$ so it will become detached if $g > \frac{1.5\gamma}{\Delta\rho a^2}$. Typically $\gamma \sim 0.1$ N/m for aqueous etches, $\Delta\rho \approx 10^3$ kg/m³ so if $g \approx 10^4$ m/s² particles down to 100 μ m will be removed. Even if a surfactant is used to decrease surface tension effects, removal is far short of the micron sized particles which are, for example, of importance in the etching of aluminium silicon copper.

However if the substrate face is angled to the direction of gravity, a particle may be dragged across its surface by a component of its own weight and thus removed. The particle is still pressed against the substrate by surface tension, so if it slides, frictional forces (equal to the surface tension force multiplied by the coefficient of friction) must be overcome. This may be an order of magnitude less than the surface tension force. Particles may also move by rolling. Apart from the movement across the sample it is also possible that in the course of movement that liquid will penetrate completely under the particle in which case it will no longer be held on by surface tension forces and will be free to fall away from the surface.

APPENDIX 2

SOURCES OF ERROR IN CENTRIFUGAL ETCH EXPERIMENTS

Sources of error and uncertainty during the experiment could be divided into the two categories below.

(1) Causes of differences in etch rate between pairs of etched samples

- i We assumed that both samples experienced virtually identical temperature histories.
- ii We estimate that the difference in etch time between pairs of samples to be ± 10 s maximum.

(2) Uncertainties in the determination of absolute etch rate

- i The exact nature of the temperature history is uncertain but its end points are given.
- ii Running the centrifuge up and down typically took 3 minutes during which the samples etched under indeterminate or normal 'g'.
- iii We estimate that the uncertainty in the determination of the exact etch time to be ± 20 s maximum.

Two samples centrifugally etched at different times under identical conditions showed etch depths at the centre of the $400\text{ }\mu\text{m}$ hole which were the same to within 2% so the reproducibility of the experiment is quite good.

APPENDIX 3

THE THEORY OF ETCHING IN A STRONG ELECTRIC FIELD

In this appendix we consider exploiting the effects of the application of an ac electrical field during resist development. Firstly, we consider the possibility of exploiting the variation in polarisability away from the interface. The energy associated with a sphere of material of radius a and dielectric constant ϵ_s in a medium of dielectric constant ϵ_m is $V_0 = 6\pi(\epsilon_s - 1) E_0^2 a^3 / (2 + \epsilon_s/\epsilon_m)$ where E_0 is the electric field in the medium. Thus the force on the sphere =

$$V_0 \frac{2}{E_0} \frac{dE}{dz} + \frac{\epsilon_s}{\epsilon_m^2 (2 + \epsilon_s/\epsilon_m)} \frac{d\epsilon_m}{dz}.$$

Depending on the geometry, E_0 varies from being independent of ϵ_m to being inversely proportional to it. In the latter case,

$$\text{Force} = V_0 \frac{d\epsilon_m}{dz} \frac{\epsilon_s}{\epsilon_m^2 (2 + \epsilon_s/\epsilon_m)} - \frac{2}{\epsilon_m}$$

The dielectric constant of the medium will depend on the amount of material dissolved in it so

$$\text{Flux} = D \frac{dn}{dz} + \frac{nV_0}{kT} \frac{d\epsilon_m}{dn} \frac{dn}{dz} f(\epsilon_s, \epsilon_m, \text{geometric factors})$$

$f(\epsilon_s, \epsilon_m) \approx 1$ so the flux is modified by a factor $\frac{nV_0}{kT} \frac{d\epsilon_m}{dn}$. If we consider a solvated species diffusing and take $E = 10^6$ V/m, $a = 3 \times 10^{-10}$ m, $\epsilon_s = 40$, $\epsilon_m = 80$, $n = 10^{27}$ m⁻³, $d\epsilon_m/dn = 10^{-27}$ m⁻³, the flux is modified by a factor $\approx 2 \times 10^6$. Thus an ac electric field should dramatically increase the etch rate but the direction of etching is still determined largely by the concentration gradient, so etch rates will be enhanced but not anisotropy. The current density is also likely to be prohibitively large in the case of inorganic etches.

The second possibility is that variations in dielectric constant in the presence of a strong ac electric field will lead to convection. A volume of material of changed dielectric constant is likely to develop over areas where etching is occurring, and this liquid will be subject to a force $\frac{d}{dz} (\epsilon E^2/2)$. Depending on geometry, the electric field may range from

being independent of E to being inversely proportional to it. Making the latter assumption, force per unit volume $\approx -E^2 \epsilon_0 / 2 (d\epsilon/dz)$ so the dimensionless quantity known as the Rayleigh number (Ra) becomes

$$\frac{E_o^2 \epsilon_o \ell^3}{2\eta D} \frac{d\epsilon}{dz}$$

(by modification of Ra for a gravitational field found by dimensional analysis).

If $E_o = 10^6$ V/m, $\epsilon_o = 8.9 \times 10^{-12}$ F/m, $\eta = 10^{-3}$ N s/m², $D = 10^{-9}$ m/s and $d\epsilon/dz = 10^4$ (0.01 drop in 1 μ m), convective flow driven by the electric field will dominate for values of $\ell > 10$ μ m. This is no better than the effect achieved by using high gravitational fields.

The third effect is particle removal. In the presence of a large electric field a particle resting on the surface will tend to charge up with charge of the same sign as that on the surface on which it is resting. If the particle has an area a and the etch a dielectric constant ϵ , the charge per unit area on the body will be $\epsilon\epsilon_o E_o$ and the force $\epsilon\epsilon_o E_o^2 A$. If a spherical particle of radius a is assumed, surface tension $2\pi a\gamma$ so the particle will be detached if $\pi a^2 \epsilon\epsilon_o E_o^2 > 2\pi a\gamma$. It therefore follows that detachment will occur if

$$a > \frac{2\gamma}{\epsilon\epsilon_o E_o^2}$$

If $E_o = 10^6$ V/m, $\epsilon = 80$ and $\gamma = 0.1$ N m⁻¹, $a > 0.3$ mm so this is not very effective.

In the light of the above calculations, we decided to investigate the effects of a dc field only.

SYSTEM		STATIC ETCH					COMPETITIVE ETCH					Significant Difference in Etch Rate Between Diff. Orientations of Sample	Flow Pattern Observed on Etched Substrate
Substrate	Etch	Etch Depth (μm)	Etch Time (min)	Etch Rate (μm/min)	Temp (°C)	Estimate of activation energy (kJ/mole)	$\frac{D^2}{t}$ 10 ⁻⁴ m ² /s	Etch Depth (μm)*	Etch Time (min)	Etch Rate (μm/min)	Temp (°C)		
Silicon (100) p-type 0.01 Ω cm	100% etch 1 vol part HF (40%) 3 vol part H ₂ SO ₄ (conc) 8 vol part acetic acid (glacial)	32 ± 3	60 ± 0.1	0.53 ± 0.05	20 ± 0.5	36 ± 8	1.6 ± 1.9	85 ± 1	32 ± 0.5	2.6 ± 0.1	23.0 ± 0.5	/	/
		49 ± 4	60 ± 0.1	0.82 ± 0.07	29 ± 0.5						29.0 ± 0.5		
Gallium Arsenide	15:1:2* etch 5 vol parts H ₂ PO ₄ (conc) 5 vol parts H ₂ SO ₄ (conc) 2 vol parts H ₂ O ₂ (30%)	11 ± 1	15 ± 0.1	0.81 ± 0.07	21 ± 0.5	Not known	1.4	50 ± 5	15 ± 0.5	3.7 ± 0.4	22 ± 0.5	/	/
Silicon Dioxide (Pyrex glass)	20% HF	17 ± 0.3	79 ± 0.1	0.40 ± 0.01	18 ± 0.5	34 ± 4	1.1	40 ± 1	46 ± 0.5	0.87 ± 0.02	21.0 ± 0.5	X	X
		28 ± 0.7	28 ± 0.1	1.00 ± 0.02	29 ± 0.5						28.0 ± 0.5		
Aluminum Silicon Copper ME 15 alloy 93.3% Al 4.6% Cu 0.7% Si 0.7% Mg 0.7% Mn	22% a1 phosphoric acid (89%) 4% acetic acid (glacial) 9% H ₂ SO ₄ (conc) 1% H ₂ O ₂ (conc) 2% 2% soln of "fluorad" (surfactant)	6 ± 0.1	131 ± 0.1	0.049 ± 0.001	21 ± 0.5	98 ± 15	1.6 ± 1.9	20 ± 1	13.0 ± 0.5	0.15 ± 0.01	22.0 ± 0.5		
		16 ± 0.3	130 ± 0.1	0.125 ± 0.002	28 ± 0.5						32.0 ± 0.5	X	X

TABLE 1

ETCH SYSTEMS INVESTIGATED

Notes: * Measured from 400 μm wide hole or line on face up angled sample.
 † These are the temperatures at the beginning and end of the etch.

The depth of the patterns in the masking layer were as follows for each substrate:

Silicon 2.5 μm
 Gallium Arsenide 0.6 μm
 Silicon Dioxide 0.2 μm
 Aluminum/Silicon/Copper 0.5 μm

The etch depths in the table do not include the mask depth.

TABLE 2

BÉNARD CELL SIZES in the HNA/Silicon System

Measured from the face down orientation

Time of Etch (min)	T (°C)	Depth of Etch (1000 μm hole)	$\frac{g^*}{(m/s^2)}$	Minimum Bénard Cell Diameter (μm)	Maximum Bénard Cell Diameter (μm)
32	22-29	60	1.9×10^4	5 (50 μm lines)	180 ⁽¹⁾ (1 mm hole)
60	19-28	134	1.9×10^4	5 ⁽²⁾ (20 μm lines)	25 (1 mm hole)
60	19-23	83	7.6×10^2	25 (1 mm hole)	190 (1 mm hole)

(1) Overall range in height of feature 2 μm (2) Overall range in height of feature 0.1 μm

TABLE 3 ETCH DEPTH FOR VARIOUS SAMPLE ORIENTATIONS WITH HNA/SILICON SYSTEM

Orientation of Sample Face	Time of Etch (min)	Value of 'g' (m/s^2)	Temp Range During Etch ($^{\circ}C$)	Diameter of Hole (μm)			
				1000	400	200	100
(A) 1) Face up angled	12	1.6×10^4	22-25	17.5 19.0 16.5 9.0	18 19 17 18	19 20 18 20	20 20 19 20
	2) Face up	-	-	22 22 26 26	26 24 25 24	25 24 25 26	27 27 27 27
(B) 1) Face up angled	32	1.6×10^4	23-29	80 78 87 85	89 87 88 87	86 84 84 86	
	2) Face up	-	-	75 74 66 64	69 66 66 66	68 64 64 67	
(C) 1) Face up angled	32	1.6×10^4	22-29		86 90 84 88		
	2) Face down	-	1.9×10^4	~59	The maximum depth of the 400 μm wide line was 76 μm		
(D) 1) Face up angled	48	1.6×10^4	19.5-24	116 109 113 105	112 116 107 109		
	2) Face down	-	-	113 116 116 114	117 113 112 116		
(E) 1) Face up angled	60	1.6×10^4	19-28	132 143 137 132	136 123 144 130 127		
	2) Face down	-	-	183 135 133 130 137	139 144 147 147		
(F) 1) Face up angled	60	6.4×10^2	19-28	98 123 89 119	111 97 120 84 76		
	2) Face down	-	-	91 82 75 76 90	100 94 102 99		

Notes:

Sample C(2) is incomplete.

The etch depths for A-C include a 2.5 μm thickness of mask whilst those for C-F include a 0.6 μm thickness of mask.

For the face up angled orientation, the topmost measurement in the circle corresponds to the depth at the points of the hole nearest to the centre of rotation of the centrifuge arm.

TABLE 4

EFFECT OF INCREASING ETCH DEPTH ON ETCH RATE

The etch depths are measured from the 400 μm holes on face up angled orientations

Etch Depth (μm)	Etch Time (min)	Etch Rate ($\mu\text{m}/\text{min}$)	Etch Temp [†] ($^{\circ}\text{C}$)
15 \pm 1	12 \pm 0.5	1.3 \pm 0.1	22-25
85 \pm 2	32 \pm 0.5	2.7 \pm 0.1	22-30
141 \pm 3	59 \pm 0.5	2.4 \pm 0.1	22-28
> 185* \pm 10	88 \pm 0.5	> 2.1	22-31

* The hole was etched all the way through.

† Values measured at the start and end of etching.

TABLE 5

ETCHING OF GaAs

Orientation	Control	Face Up	Face Down	Angled Face Up	Angled Face Down
Temperature/°C	21	22	30	30	22
g/ms ⁻²	9.8	1.5×10^4	1.77×10^4	1.5×10^4	1.77×10^4
Etch time/mins	13.33	13.0	13.33	13.33	13.08
Etch depth/ μ m is:					
1.0 mm diameter hole	12.5	19.7-28.7	15-45.5	38.2-58	40.5-44.5
0.2 mm diameter hole	12.5	20.7-23.6	14-39	49-58	45-51
0.4 mm line	12.5	19.3-26.5	57-59	42.7-51	43.4-53
0.1 mm line	12.5	21.4	57.9	42.1-44.4	44.8-47.6

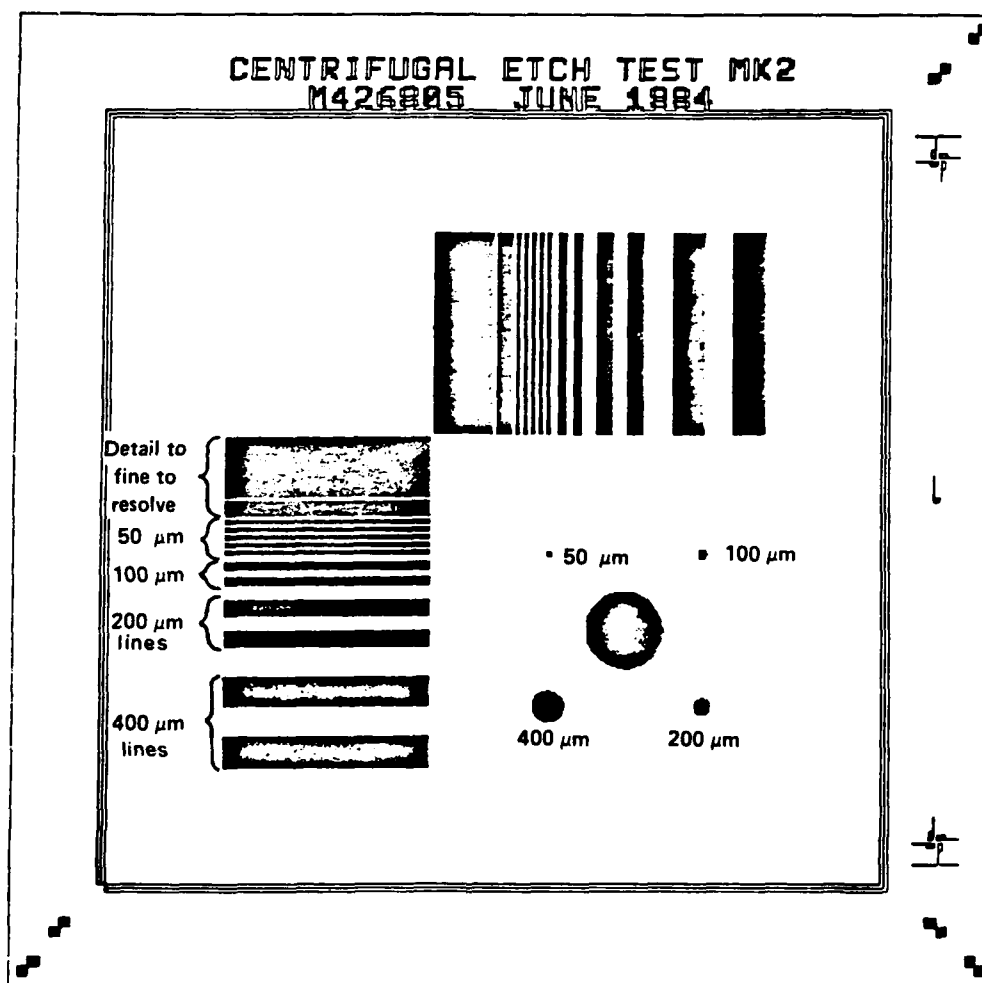


FIGURE 1

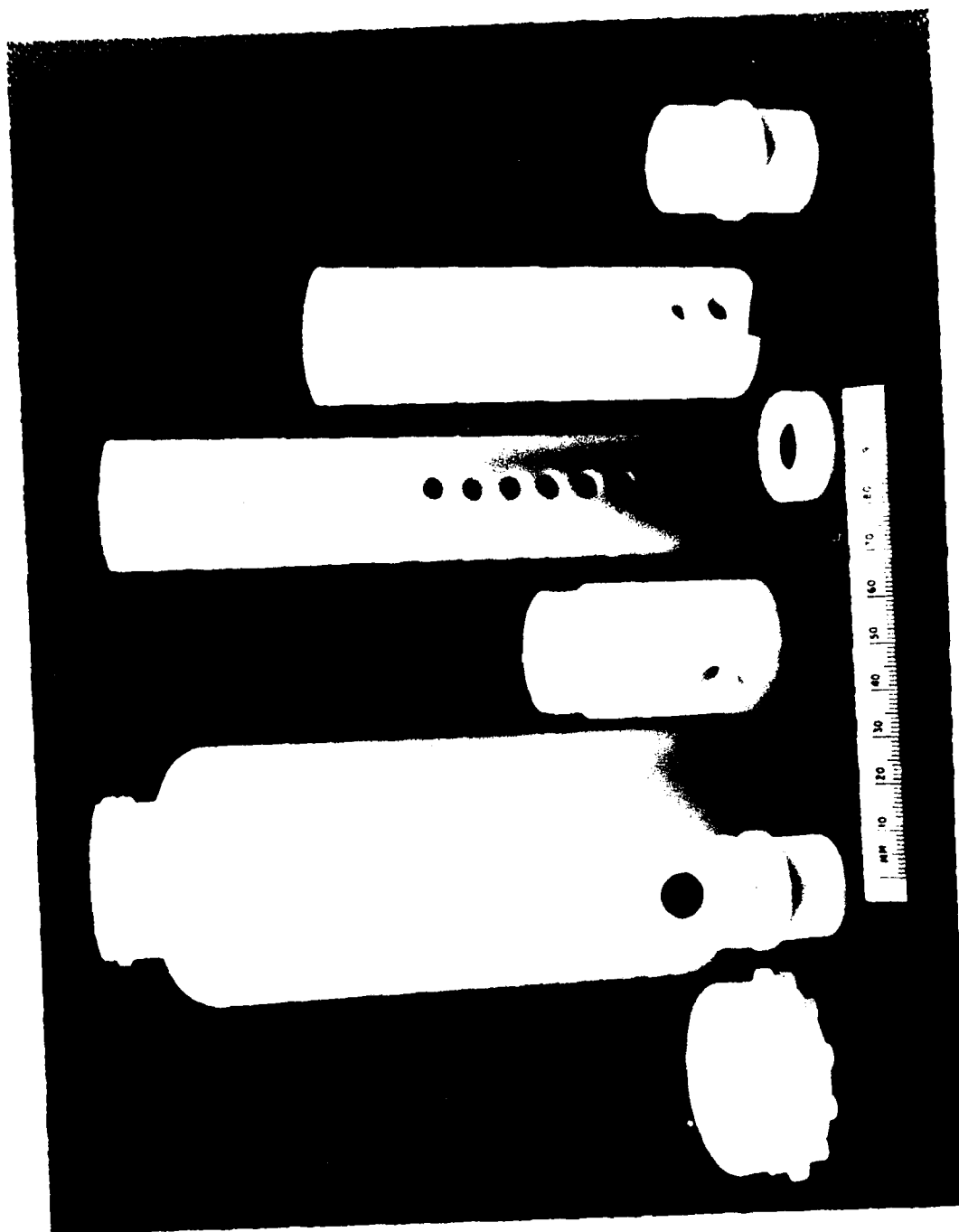


FIG 2

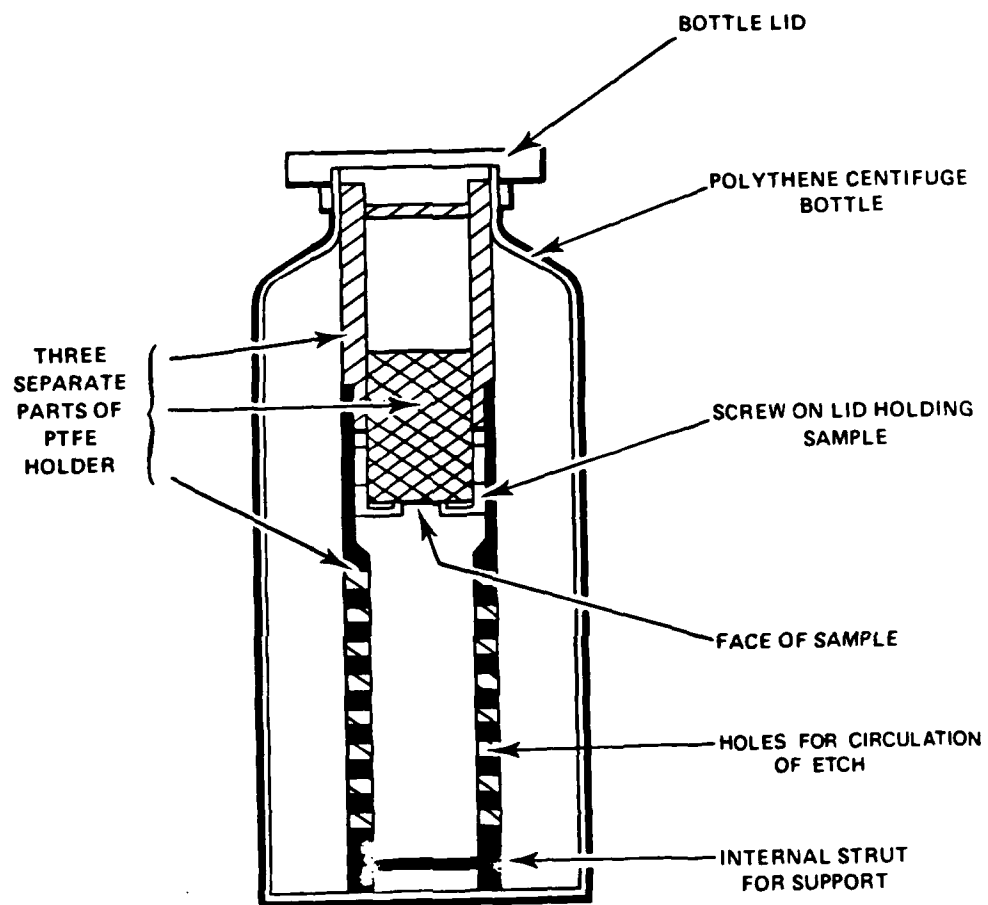
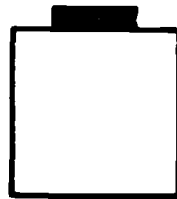


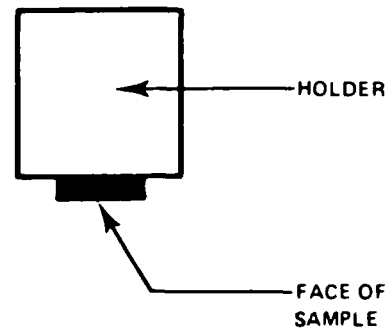
DIAGRAM SHOWS FACE DOWN ORIENTATION

FIG 3 SAMPLE IN HOLDER AND BOTTLE

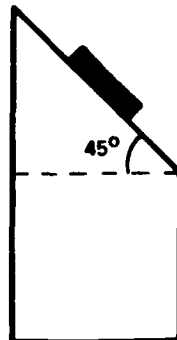
(a) FACE UP



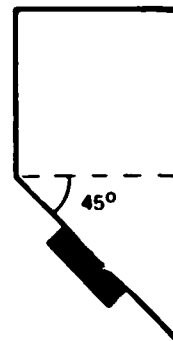
(b) FACE DOWN



(c) FACE UP ANGLED



(d) FACE DOWN ANGLED



DIRECTION
OF
GRAVITATIONAL
FIELD

FIG 4 ORIENTATIONS OF SAMPLE RELATIVE TO GRAVITY

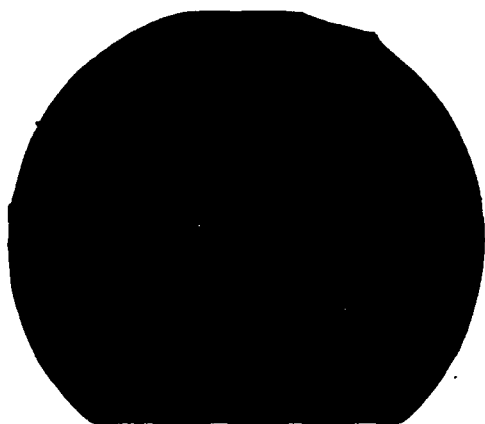


FIGURE 5

Silicon/HNA system
 $g = 9.8 \text{ m/s}^2$
 Etched 60 mins at 30°C

1 mm diameter hole
 Etched depth $\sim 40 \mu\text{m}$

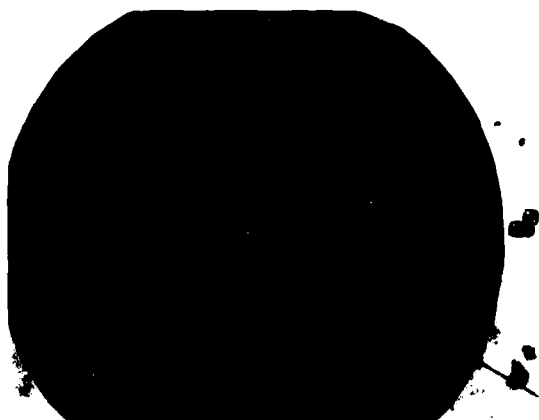


FIGURE 6

Silicon/HNA system
 $g = 1.6 \times 10^4 \text{ m/s}^2$
 Face up angled
 Etched 32 mins at $22-29^\circ\text{C}$

1 mm diameter hole
 Etched depth $\sim 90 \mu\text{m}$

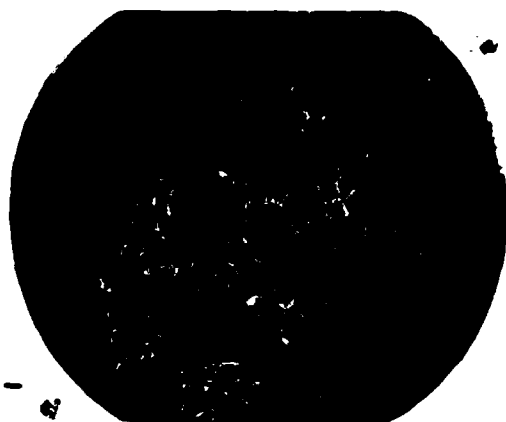


FIGURE 7

Silicon/HNA system
 $g = 1.9 \times 10^4 \text{ m/s}^2$
 Face down
 Etched 32 mins or $22-29^\circ\text{C}$
 1 mm diameter hole
 Etched depth $\sim 60 \mu\text{m}$



FIGURE 8

Silicon/HNA system
 $g = 1.9 \times 10^4 \text{ m/s}^2$
 Face down
 Etched 60 mins at 19.28°C

1 mm diameter hole
 Etched depth $130 \mu\text{m}$



FIGURE 9

Silicon/HNA system
 $g = 1.9 \times 10^4 \text{ m/s}^2$
 Face down
 Etched 32 mins at 22.29°C
 $50 \mu\text{m}$ lines
 Etch depth $60 \mu\text{m}$



FIGURE 10

Silicon/HNA system
 $g = 1.9 \times 10^4 \text{ m/s}^2$
 Face down
 Etched 60 mins at 19.28°C
 $20 \mu\text{m}$ lines
 Depth of etch $\sim 130 \mu\text{m}$



FIGURE 11

Silicon/HNA system

$g = 7.6 \times 10^2 \text{ m/s}^2$

Face down

Etched 60 mins at $19 \pm 2^\circ\text{C}$

Depth of etch $80 \mu\text{m}$



FIGURE 12

Silicon etched HNA 32 mins 23 29°C
 Face up angled
 $g = 1.6 \times 10^4 \text{ ms}^{-2}$
 200 μm wide line
 Lateral etch depth = $58 \pm 4 \mu\text{m}$
 Vertical etch depth = $87 \pm 2 \mu\text{m}$



FIGURE 13

Silicon etch in HNA

(a) Face up 32 mins 23 29°C
 $g = 1.6 \times 10^4 \text{ ms}^{-2}$
 200 μm line (LHS)
 Lateral etch depth = $51 \pm 4 \mu\text{m}$
 Vertical etch depth = $69 \pm 3 \mu\text{m}$



(b) Face down 32 mins 22 29°C
 $g = 1.9 \times 10^4 \text{ ms}^{-2}$
 200 μm line (LHS)
 Lateral etch depth = $56 \pm 4 \mu\text{m}$
 Vertical etch depth = $60 \pm 2 \mu\text{m}$

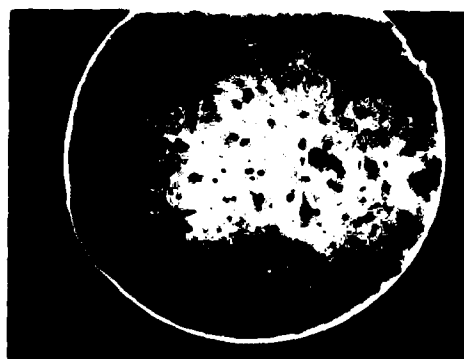
(a) Control. 13 mins 21°C



(b) Face up angled. 30°C $1.5 \times 10^4 \text{ ms}^{-2}$ 13 mins



(c) Face down. 22°C $1.77 \times 10^4 \text{ ms}^{-2}$ 13 mins



(d) Face down angled. 30°C $1.77 \times 10^4 \text{ ms}^{-2}$ 13 mins

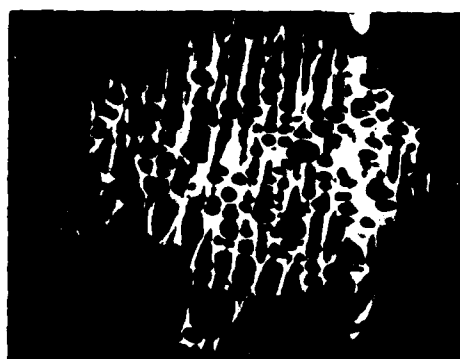
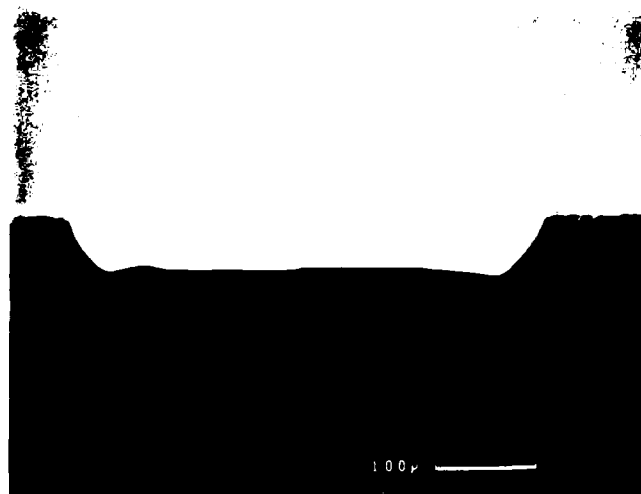


FIG 14 OPTICAL MICROGRAPHS OF ETCHED GaAs

(a) Etched for 13.33 mins at 30°C and $1.77 \times 10^4 \text{ ms}^{-2}$ in face down orientation

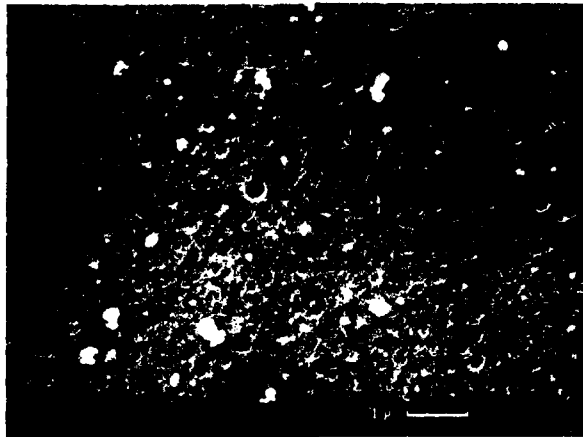


(b) Etched for 13.33 mins at 30°C and $1.5 \times 10^4 \text{ ms}^{-2}$ in angled face up orientation. The left hand side of the micrograph was "uphill"



FIGURE 15 CROSS SECTION SCANNING ELECTRON MICROGRAPHS OF ETCHED GaAs

(a) Static control $g = 9.8 \text{ ms}^{-2}$. Etched 8 mins 19.4°C . Etched depth = $0.5 \mu\text{m}$



(b) Angled face up $g = 1.5 \times 10^4 \text{ ms}^{-2}$. Etched 8 mins 19.7°C . Etched depth = $0.5 \mu\text{m}$



(c) Angled face down $g = 1.77 \times 10^4 \text{ ms}^{-2}$. Etched 8 mins 19.7°C . Etched depth = $0.5 \mu\text{m}$

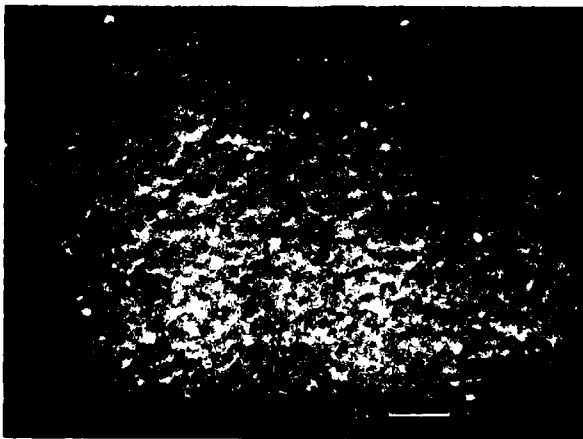
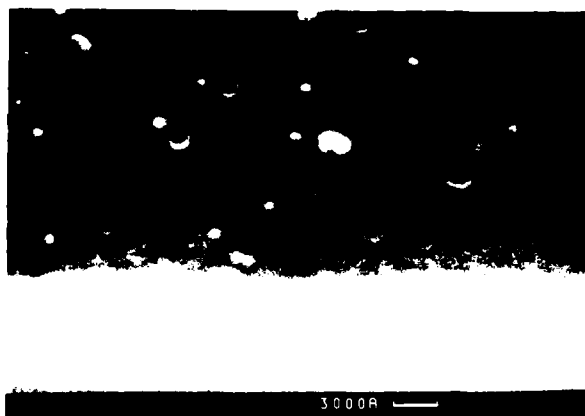


FIGURE 16 PARTICULATE REMOVAL FROM ALUMINIUM : SILICON : COPPER

- (a) Face down angled. Etched 8 mins at 19.7°C and $1.77 \times 10^4 \text{ ms}^{-2}$. "Up field" side of a $400 \mu\text{m}$ width line



- (b) "Down field" edge of the feature shown in (a)



- (c) Face up angled $g = 1.5 \times 10^4 \text{ ms}^{-2}$. Etched 8 mins 19.7°C . Note the concentration of particles in the pits



FIGURE 17 EVIDENCE FOR PARTICLE MIGRATION

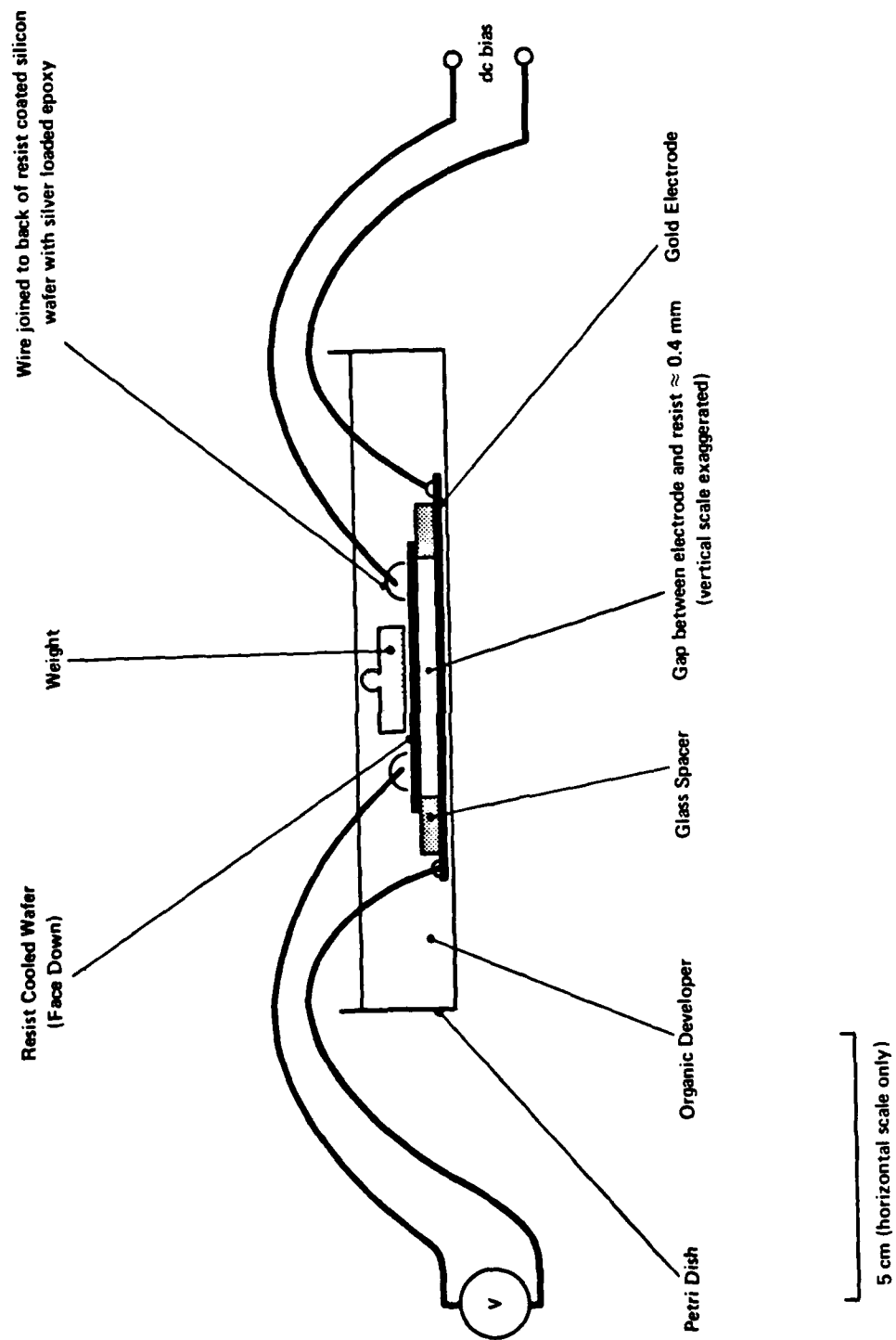


FIGURE 18 WAFER UNDER DEVELOPMENT IN AN ELECTRIC FIELD

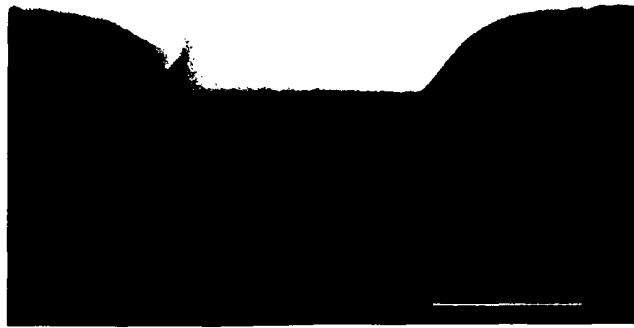


FIGURE 19 PMMA RESIST. CONTROL DEVELOPED 70S AT 18°C. 2 μ m WIDE LINE



FIGURE 20 PMMA RESIST. SAMPLE A, GOLD ELECTRODE WAS POSITIVE PLATE, DEVELOPED 70S AT 18°C. 2 μ m WIDE LINE



FIGURE 21 PMMA RESIST. SAMPLE (B). RESIST COATED WAFER WAS POSITIVE PLATE, DEVELOPED 70S AT 18°C. 20 μ m WIDE LINE

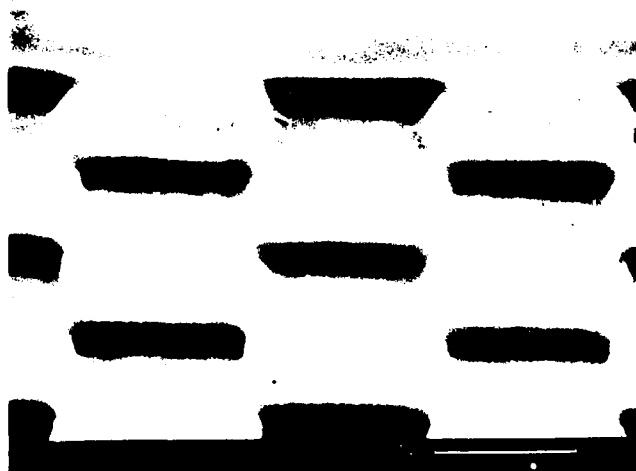


FIGURE 22 PMMA RESIST. SAMPLE A. GOLD ELECTRODE WAS POSITIVE PLATE, DEVELOPED 70S AT 18°C. 3 μ m SIDE SQUARES

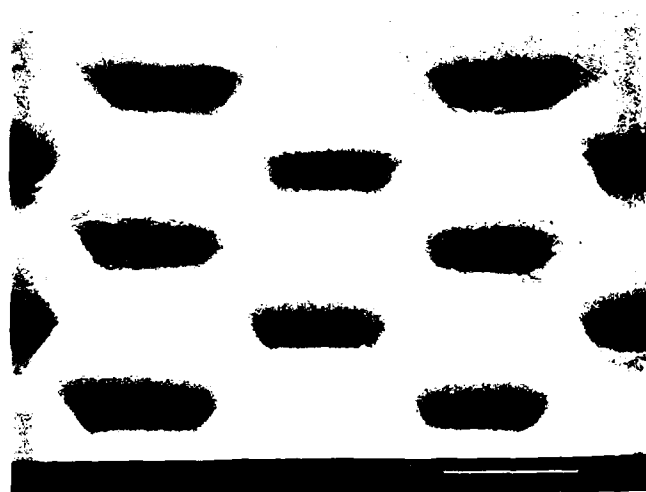


FIGURE 23 PMMA RESIST. SAMPLE B. RESIST WAFER WAS POSITIVE PLATE, DEVELOPED 70S AT 18°C. 3 μ m SIDE SQUARES

END

DATE
FILMED

7-87